

## Research

# Production of glass ceramic from rice husk and periwinkle shells

B. Aremo<sup>1</sup> · D. A. Isadare<sup>1</sup> · O. E. Akinduro<sup>1</sup> · O. E. Bello<sup>1</sup> · M. O. Adeoye<sup>1</sup> · S. A. Ayodeji<sup>2</sup> · G. F. Abass<sup>3</sup> · K. M. Oluwasegun<sup>4</sup>

Received: 19 November 2023 / Accepted: 28 February 2024

Published online: 03 March 2024

© The Author(s) 2024 [OPEN](#)

## Abstract

Glass ceramic was produced by replacing the major glass forming materials, silica and calcium oxide, with derivatives from rice husk and periwinkle shells respectively. Glass formulation comprising of silica extracted from the rice husk and calcium oxide from powdered calcined periwinkle shells were compounded with analytical grade sodium carbonate. Silica was extracted from rice husk and characterized using XRD. SEM/EDS of the periwinkle shell revealed a structure dominated by calcium and oxygen; however, there was a significant presence of magnesium. Glass ceramic was produced by melting the mixture at 1300 °C followed by melt quenching. FTIR of the material showed the presence of the carbonyl functional group, calcium oxide, magnesium oxide and various bond configurations of silica. SEM of the glass ceramic showed sparsely distributed particles of the crystalline phase, while XRD revealed the presence of 55% amorphous phase. Several crystalline phases were present, dominated by polymorphs of silica such as quartz (22.15 wt.%) and cristobalite (5.68 wt.%). Also present are mullite (5.58 wt.%), calcite (1.95 wt.%) and Wollastonite (6.86 wt.%). Noticeable in the crystalline phase is Whitlockite (2.33 wt.%), a magnesium and phosphorus rich animal-source bio ceramic, traceable to the periwinkle which may impart some bioactivity to the material.

**Keywords** Rice Husk · Periwinkles · Glass Ceramics · Glass · Sustainability

## 1 Introduction

The invention of glass making is often credited to the Phoenicians at around 5000 BC [1], and its continued relevance is due to its inertness, excellent barrier properties, and formability into different shapes and sizes. Glass has been subject to a plurality of definitions that reflect the various perspectives from which it is viewed. It would seem more appropriate however to reserve the term “glasses” only for those non-crystalline solids that exhibit the phenomenon of a “glass transition” [2]. Glass continues to enjoy growing importance in today’s world, with a annual global glass production of about 150 million tons in 2019 [3].

Glass ceramics are siliceous glasses with a substantial crystalline phase comprising of various oxides. They are attractive for different applications due to their often-superior properties over conventional glasses. Such applications include

---

✉ B. Aremo, baremo@oauife.edu.ng; D. A. Isadare, disadare@oauife.edu.ng; O. E. Akinduro, akinduroolumide@gmail.com; O. E. Bello, bellooluwatosin1@gmail.com; M. O. Adeoye, madeoye@yahoo.com; S. A. Ayodeji, sodrudeenayodeji278@gmail.com; G. F. Abass, abass.gbemi@gmail.com; K. M. Oluwasegun, excetom@gmail.com | <sup>1</sup>Department of Materials Science and Engineering, Obafemi Awolowo University, Ile-Ife, Nigeria. <sup>2</sup>Matrix Energy Group, Lagos, Nigeria. <sup>3</sup>Department of Materials Science and Engineering, College of Mechanics and Material, Hohai University, Nanjing, China. <sup>4</sup>Department of Materials Science and Engineering, University of Manitoba, Manitoba, Canada.



electronics (microelectronic packing), medicine and dentistry (bio glass ceramics implants, bone and in dental prostheses) and optical materials [4].

Glass ceramics have the same basic composition as glass, but typically differ in percentage of crystalline volume. Glass ceramics can have up to 95–98 volume percent crystalline phase, with only a small percentage vitreous phase. However, the extent of crystallinity and grain boundaries reduces the transparency of the material [5]. MAS ( $\text{MgO-Al}_2\text{O}_3\text{-SiO}_2$ ) transparent glass–ceramics have attracted the most attention due to their excellent physical and chemical properties [6].

Rice (*Oryza sativa*) is a major staple food for more than half of the world's population and it is farmed in more than 100 countries [7]. It is the world's third-most produced agricultural crop with 756 million tons produced globally in 2019 [8]. Rice production however leads to large volume of rice husk as a waste material which accounts for about 20% of the production volume [9].

Rice husk contains 75–90% organic matter such as cellulose and lignin, with the remainder being silica, alkalis, and trace elements [10]. However, after calcination, rice husk ash is 87–97% silica; the presence of high proportion of silica makes it an industrially interesting material [11]. Despite the massive amount of annual production worldwide, so far rice husk has been recycled only for low value applications [12]. Currently, it is being used locally as a fuel, as additives in kilns and furnaces bricks [13]; it is also used as fertilizer and substrate [14].

In Nigeria, periwinkles (*Tympanotonus fuscatus* var *radula*) are commonly found in most coastal communities, and it is especially popular in the Niger Delta areas in the South-South and costal communities in the South-West zones of the country. In these communities, periwinkle is widely consumed and is a relatively cheap source of animal protein [15]. However, the leftover shells from the consumption of periwinkles constitute a major source of environmental litter due to its non-biodegradable nature. Some efforts have been made for the utilization of periwinkle shells locally. They have been considered as partial replacement for granite in concrete [16]. Also, powdered periwinkle shells have been compounded with polymers for improved mechanical and electrical insulation properties [17]. Other reported uses include adsorption of heavy metals from wastewater and as a replacement for asbestos in brake pad [18]. It has also been used for the production of activated carbon [19]. However, despite these uses large quantity of the periwinkle shells are still simply disposed of indiscriminately in the local communities [20].

Radical solutions are needed to check the dihedral problem of steady depletion of natural reserves of industrially important raw materials, and the burgeoning volume of agricultural wastes from the consumption of popular food items. A pathway for achieving this is a “circular economy”, wherein one production sector's waste is another's raw material [21]. The trend towards sustainable production has inspired efforts to synthesize glass ceramics from agricultural and industrial waste materials, such as in Hossain et al. [22] wherein a bioactive wollastonite-base glass–ceramic was produced from rice husk ash and eggshells.

This work presents yet another pathway for a high-value utilization of the large volume of rice husk wastes produced annually from rice cultivation, and periwinkle shells leftover from the consumption of the marine snails. This was achieved by compounding rice-husk-derived silica with pulverized periwinkle shells, to produce environment-friendly and sustainable glass products.

## 2 Materials and methods

### 2.1 Materials

Rice husks were obtained from a local rice farm in Ogbese Town in Ondo State, Southwest Nigeria. Samples are shown in Fig. 1. Periwinkle shells were obtained from a dump site in a local market in Badagary, a coastal community in Lagos, Southwest Nigeria. Samples of periwinkle shells are shown in Fig. 2. Sodium hydroxide (Qualikems, India) and hydrochloric acid (Fluka, United Kingdom) were employed in the extraction of silica from rice husk.

### 2.2 Extraction of silica from rice husk

The flow diagram for the extraction of silica is presented in Fig. 3. The procedure followed the method described in the patent by Adam and Fua [23, 24]. The first step is the calcination of the rice husk at 700 °C for about 6 h, after which the resulting ash is allowed to furnace-cool to room temperature. After cooling, the rice husk ash was ground into fine powder in an agate mortar, to increase the specific surface area of the ash.

**Fig. 1** Raw Rice Husks**Fig. 2** Periwinkle Shells

Rice husk ash is boiled in 1 M of sodium hydroxide solution, with constant stirring for about 1 h. This process causes the silica in the ash to react with the sodium hydroxide to give a sodium silicate solution, with significant ash residue present. This resultant solution is filtered, using filter paper, producing a filtrate of clean sodium silicate solution. Silica gel is precipitated by adding 1 M hydrochloric acid to the sodium silicate filtrate which was allowed to age for about an hour. The silica gel was oven-dried at about 700 °C to burn off any organic impurities.

### 2.3 Production of glass ceramic

The glass ceramic was composed of 70 wt. % rice husk derived silica, 15 wt. % calcined crushed periwinkle shells and 15 wt. % anhydrous sodium carbonate. This was based on a simple soda-lime glass composition suggested by Bauccio [25]. Rice husk derived silica and crushed periwinkle shells powder were used to directly substitute for silica and calcium oxide respectively. The analytical grade anhydrous sodium carbonate (Qualikems, India) thermally decomposes to give sodium oxide. The constituent materials for the production of the glass were thoroughly mixed together in a mortar. They were heated to 1300 °C in a Carbolite RHF 1600 chamber furnace, for 1 h, after which the melt was brought out (see Fig. 4) and molten glass was scooped out with stainless steel spatula, forming glass beads.

**Fig. 3** Process flow diagram for the extraction of silica from rice husk

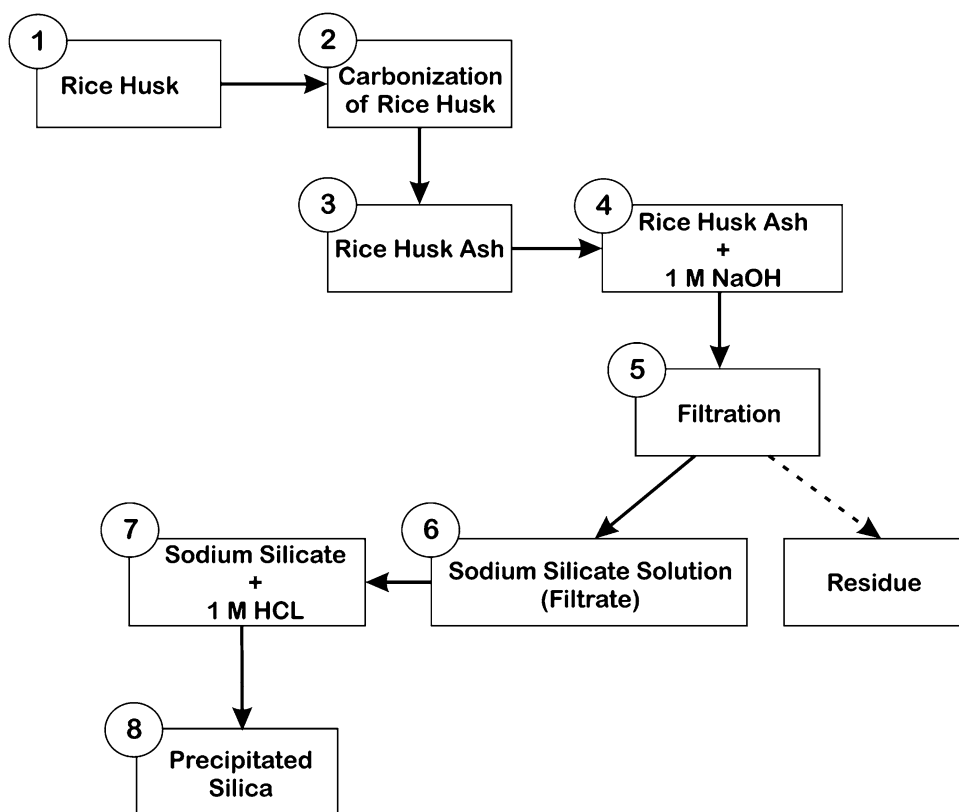


**Fig. 4** Molten glass beads



## 2.4 Characterization of materials

Characterizations were carried out on the precursor materials and the glass ceramic. Scanning electron microscopy (SEM) and energy dispersive x-ray spectroscopy (EDS) were carried out for structural and elemental identification using Carl Zeiss Smart Evo 10 Scanning Electron Microscope. This was done on the rice husk, rice husk ash and glass ceramic. X-ray diffraction (XRD) was carried out on the raw rice husk derived silica and glass ceramic on Shimadzu XDS 2400H diffractometer with CuK $\alpha$  X-rays (wavelength,  $\lambda = 1.54056 \text{ \AA}$ ). Fourier Transform Infrared (FTIR) Spectroscopy was done on the glass ceramic to investigate its composition and nature of its chemical bonds with Agilent Technologies Cary 630 spectrometer.

### 3 Results and discussions

#### 3.1 SEM of rice husk and rice husk ash

The SEM image of the rice husk is presented in Fig. 5. The rectangular cellular structure of the rice husk grains is discernable, appearing in rows in a lamellar pattern. Intergranular cracks and de-laminations are noticeable between the grains, apparently caused by loss of moisture from drying. The rice husk composition determined by EDS is presented in Table 1. The EDS spectra is presented in Fig. 6. The composition is dominated by Si (31.96 wt.%) and Oxygen (64.81 wt.%), totaling about 90 wt.% of the concentration at the location. This suggests a composition that is rich in silica. The composition of magnesium, rhenium and hafnium present is about 2.5 wt.%.

#### 3.2 Rice husk ash

The SEM image of the rice husk ash particles is presented in Fig. 7a and b. The presence of un-calcinated rice husk fragments is noticeable. This is highlighted in Fig. 7b, with the husk's lamella grain structure still discernable. This is due to

**Fig. 5** SEM micrograph of rice husk

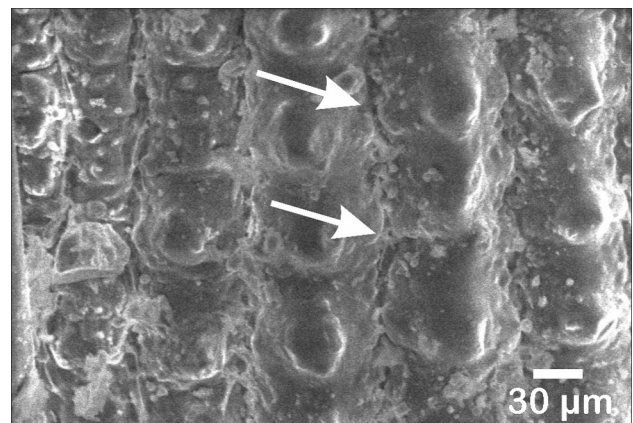


**Table 1** EDS compositional analysis of rice husk

Element	O	Mg	Si	Hf	Re
Wt.%	64.81	0.58	31.96	1.03	1.62

**Fig. 6** EDS spectra of rice husk

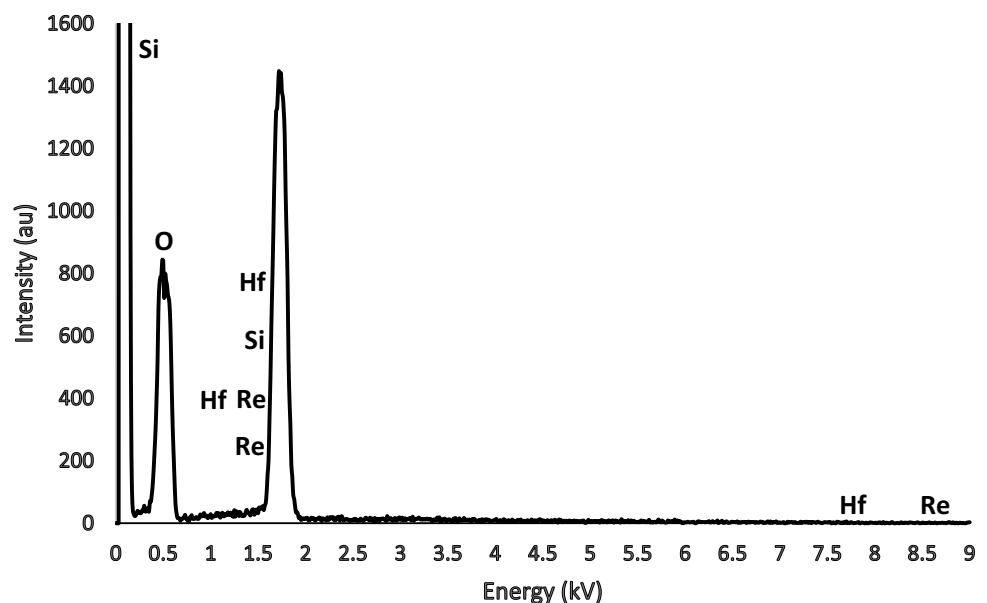
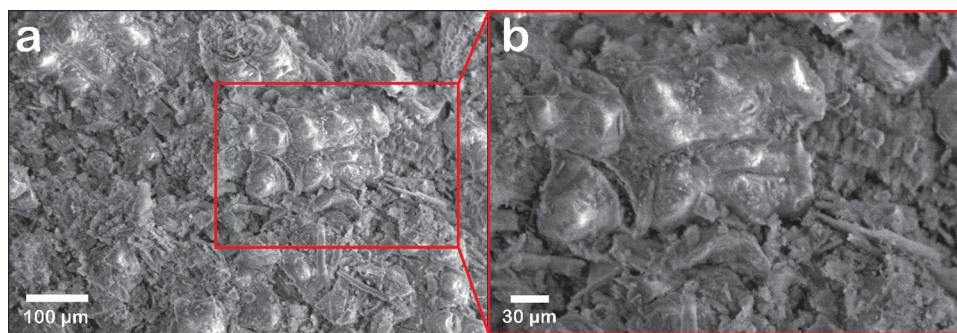




**Fig. 7** **a** and **b** SEM micrographs of rich husk ash



the absence of constant stirring during the calcination of the husk pile. This, coupled with the low thermal conductivity of the husk meant that husk particles deep inside the husk pile were shielded from the high calcination temperature. The EDS spectra of the rice husk is presented in Fig. 8 while the corresponding compositional analysis is presented in Table 2. The table shows a concentration of Si of 32.50 wt.% and O of 62.75 wt.%. This confirms the presence of high concentration of silica.

### 3.3 XRD of rice husk silica

The silica extracted from the rice husk after following the steps outlined in the flow chart in Fig. 3 is presented Fig. 9. It is snow-white in appearance after drying the gel precipitated in step 8 of Fig. 3. Figure 10 shows the XRD pattern of the silica. The peaks at  $2\theta$  of  $21.928^\circ$  and  $31.718^\circ$  indicate the existence of crystalline silica in the form of quartz and cristobalite respectively. Also, the peak at  $2\theta$  of  $45.00$  indicates the presence of mullite. The peak at  $2\theta$  of  $58.0$  indicates the presence of quartz. The presence of the polymorphs of silica confirms the extraction of silica from the rice husk.

### 3.4 SEM and EDS characterization of calcined periwinkle shell

The SEM image of the periwinkles shell is presented in Fig. 11. The shell texture is observed to be coarse, consisting of overlapping plates. The EDS spectra is presented in Fig. 12, while the EDS compositional analysis is presented in Table 3.

**Fig. 8** EDS spectra of rice husk ash

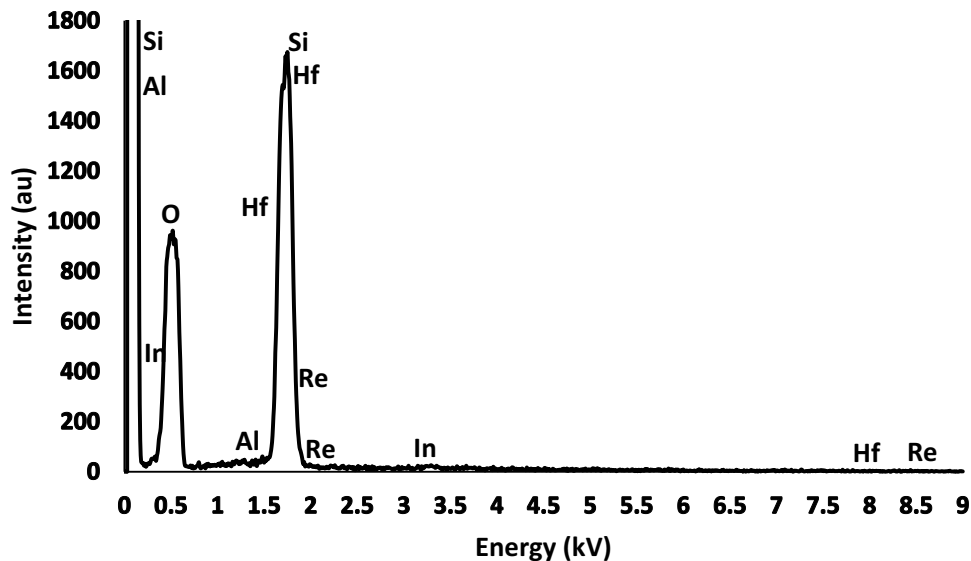


**Table 2** EDS compositional analysis of rice husk ash

Element	O	Al	Si	In	Hf	Re
Wt.%	62.75	0.55	32.50	1.38	0.99	1.83

**Fig. 9** Extracted rice husk silica



**Fig. 10** X-ray diffraction pattern of calcined rice husk silica

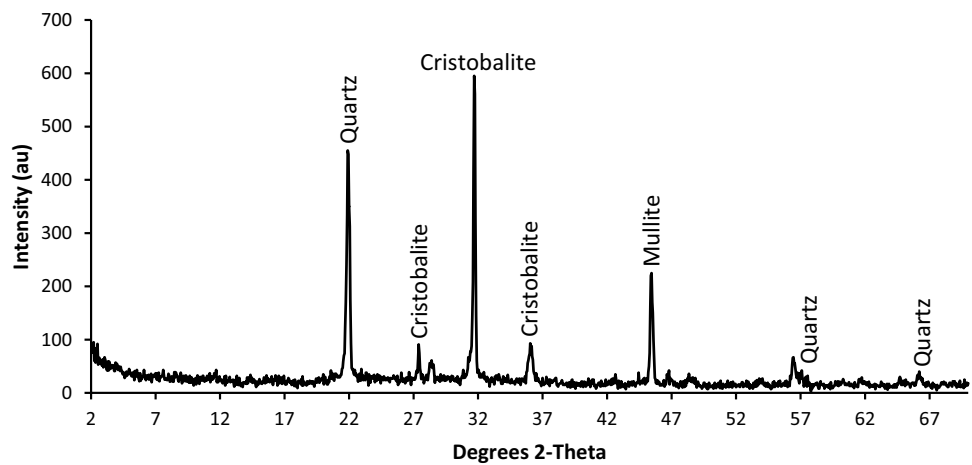
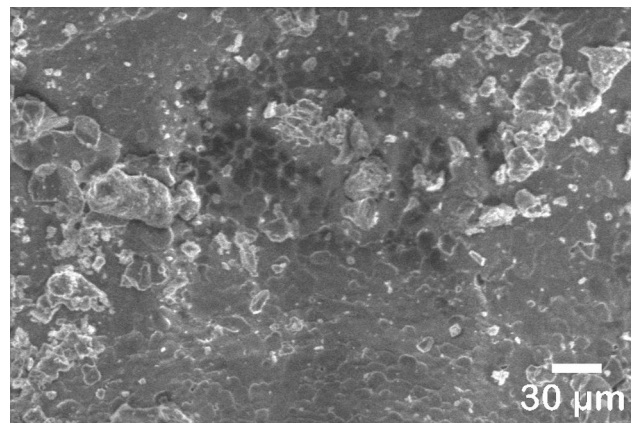


**Fig. 11** SEM micrograph of periwinkle shell



The major elements are C (22.09 wt.%), O (51.32 wt.%) and Ca (14.13 wt.%). Notable minor elements are Mg (3.77 wt.%) and Na (2.68 wt.%).

The presence of Ca, C and O suggests the presence of calcium trioxocarbonate ( $\text{CaCO}_3$ ). The presence of the minor elements Mg and Na are notable. Periwinkles are marine snails, and the shells used in this study were sourced from a coastal community on the Atlantic coast of Lagos, Nigeria. Marine organisms are exposed to elements from salt minerals that are prevalent in the ocean environment, prominent of which are Mg and Na. Magnesium salt is the second most

**Fig. 12** EDS spectra of periwinkle shell

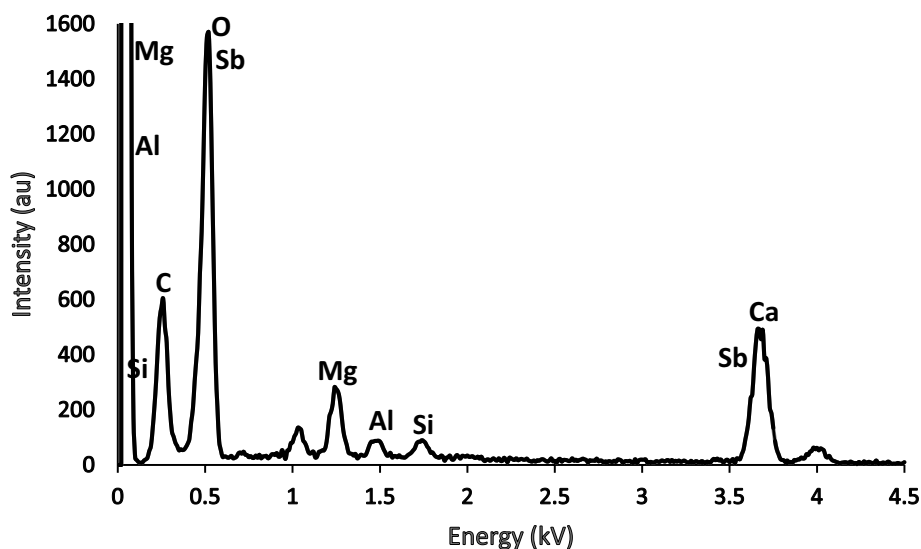


**Table 3** EDS analysis of periwinkle shell

Element	C	O	Na	Mg	Al	Si	Ca	Sb
Wt.%	22.09	51.32	2.68	3.77	0.99	0.92	14.13	4.10

plentifully salt in sea water [26] hence, its presence in the shells can be traceable to a lifetime exposure of the periwinkles to the ocean environment.

### 3.5 FTIR spectroscopy of glass ceramic

The FTIR spectra for the glass ceramic is presented in Fig. 13. From the figure, the asymmetric vibration of Si–O is observed at a wavenumber of  $1006\text{ cm}^{-1}$ . The asymmetric vibration of Si–OH at  $916\text{ cm}^{-1}$  and the symmetric vibration of Si–O at  $738\text{ cm}^{-1}$  are also noticeable. Absorption bands in the range of  $800$  and  $1260\text{ cm}^{-1}$  can be described as a superimposition of different  $\text{SiO}_2$  peaks and Si–OH bonding [27]. Also, O–Mg–O bending is noticed at  $484.5\text{ cm}^{-1}$ , similar to the findings of Choudhary et al. [28], while the peak at  $574\text{ cm}^{-1}$  shows the presence of Ca–O group.

The band region between  $1700$  and  $1725\text{ cm}^{-1}$  is indicative of strong C=O stretching [29]. Stretching vibrations generally require more energy and show absorption bands of higher wavenumbers. The peak observed at a wavenumber of  $1703\text{ cm}^{-1}$  signifies the presence of a carbonyl group in the glass. The high transmittances (from 92 to 97%) in the fingerprint region is an indication of the low impurity level in the material because there are few bonds to absorb the wavelengths in this region.

### 3.6 SEM and EDS

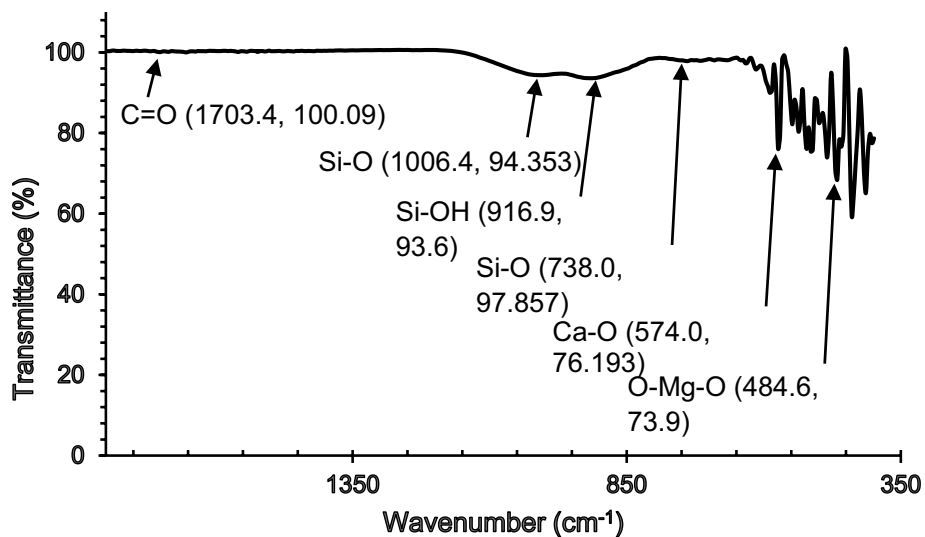
The SEM micrograph of the glass ceramic surface is presented in Fig. 14a and b. Specks of the crystalline phase can be seen festooned across the surface in Fig. 14a. These are visible in Fig. 14b (arrow A). A bubble that apparently breached the surface can be seen at arrow B (Fig. 14b). This bubble collapsed and flaked off, leaving behind a shallow pit. The crystalline phases can also be seen inside the exposed surface of the pit, beneath the surface. The EDS spectra of the glass is presented in Fig. 15, while the elemental composition is presented in Table 4. The elements identified are Si, Ca, Na, O, C and P. While Na is part of the major glass forming composition, P can be traced to the periwinkle shell.

### 3.7 XRD of glass ceramic

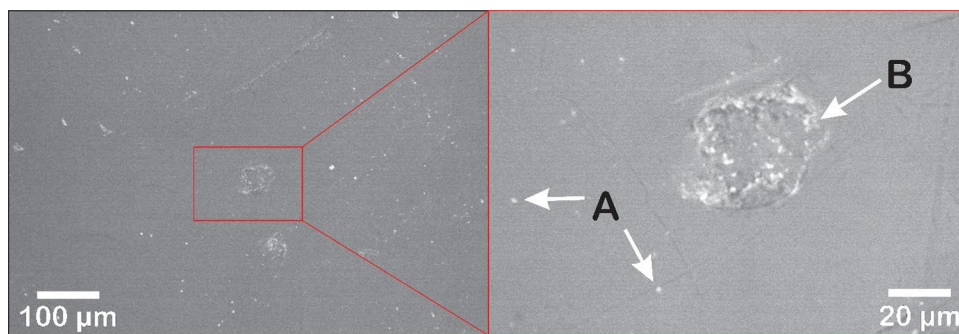
The representative XRD patterns of the glass ceramic are shown in Fig. 16, while Table 5 shows the corresponding identified phases and quantitative analysis. From the figure, the structure of glass ceramic is evident. The peaks representing the various crystalline phases are superimposed on the characteristic amorphous glass hump between  $2\theta$  of  $20$  and



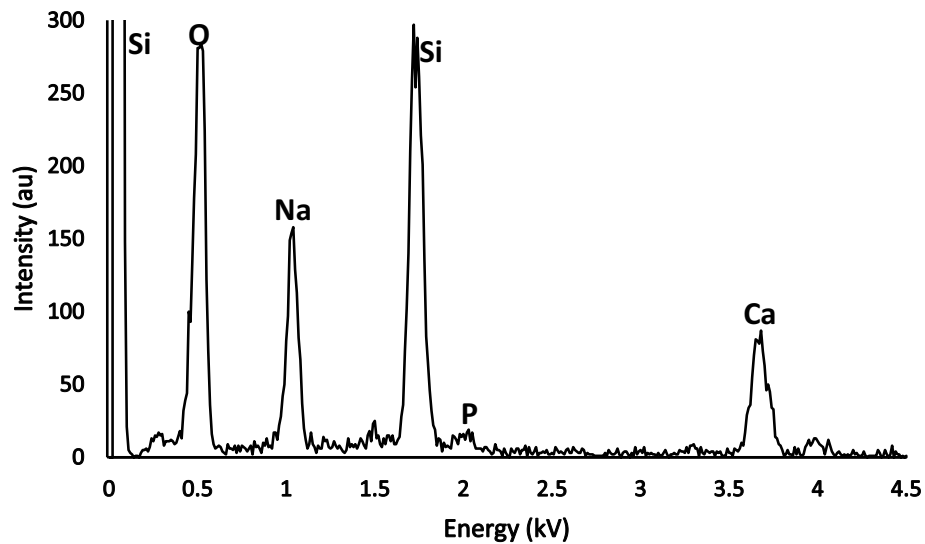
**Fig. 13** FTIR spectra of the glass ceramic



**Fig. 14 a and b** SEM micrographs of the glass ceramic

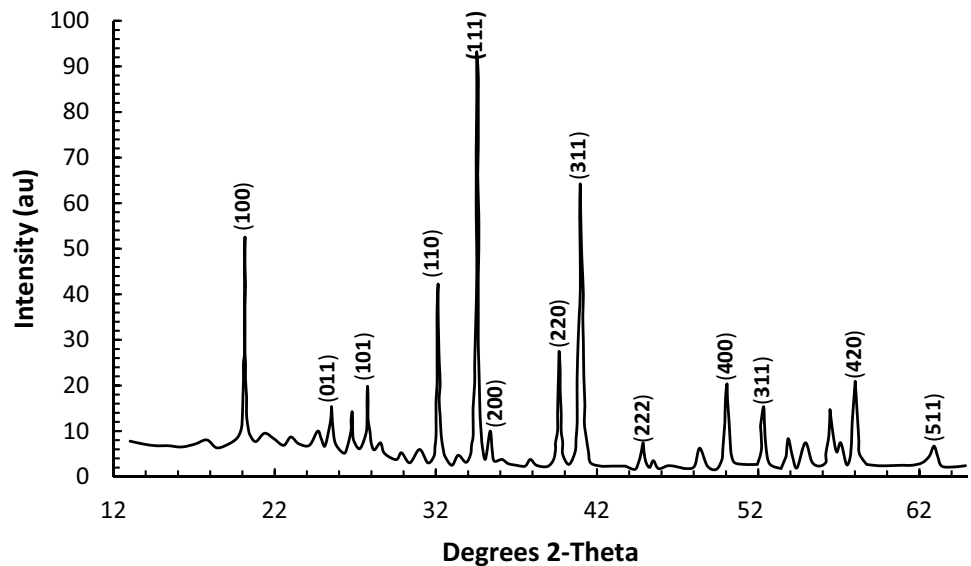


**Fig. 15** EDS of the glass ceramic



**Table 4** EDS of the glass ceramic

Elements	C	O	Na	Si	P	Ca
Wt. %	2.86	45.75	15.06	19.66	1.60	15.08

**Fig. 16** XRD of glass ceramic**Table 5** XRD compositional analysis of the glass ceramic

2θ	Plane	Intensity	d-Value (Å <sup>o</sup> )	Minerals	wt.%
20.00	1 0 0	54.71	4.4342	Amorphous	13.14
24.42	0 1 1	15.23	3.6407	Amorphous	3.66
27.83	1 0 1	21.68	3.2017	Amorphous	5.21
32.00	1 1 0	45.12	2.7933	Amorphous	10.83
34.28	1 1 1	94.11	2.6125	Amorphous	22.61
35.00	2 0 0	9.70	2.5607	Whitlockite	2.33
39.95	2 2 0	28.54	2.2541	Wollastonite	6.86
41.00	3 1 1	67.21	2.1987	Quartz	16.14
45.00	2 2 2	8.75	2.0120	Mullite	2.10
50.00	4 0 0	23.64	1.8221	Cristobalite	5.68
52.21	3 3 1	14.50	1.7500	Mullite	3.48
58.07	4 2 0	25.00	1.5865	Quartz	6.01
63.00	5 1 1	8.12	1.4737	Calcite	1.95

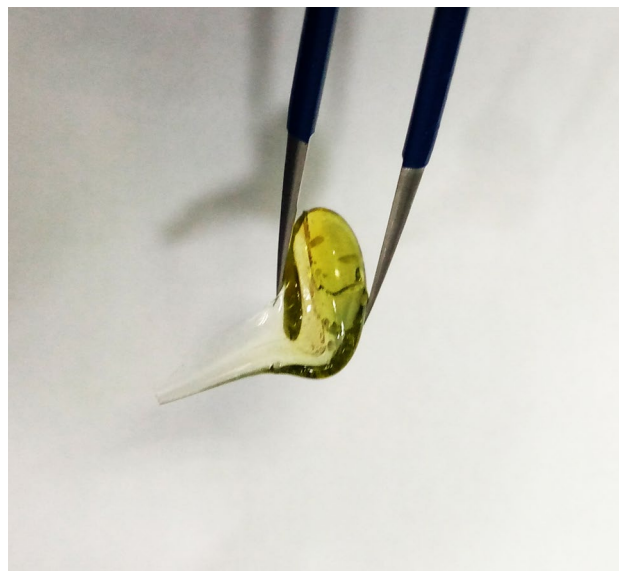
34. From Table 5, a significant amorphous phase of residual glass of 55.45 wt. % is apparent. The crystalline phases are dominated by polymorphs of silica such as quartz (22.15 wt.%) and cristobalite (5.68 wt.%).

Also present is mullite ( $3\text{Al}_2\text{O}_3\cdot 2\text{SiO}_2$  or  $2\text{Al}_2\text{O}_3\cdot \text{SiO}_2$ ) at 5.58 wt.%, and calcite ( $\text{CaCO}_3$ ) at 1.95 wt.%. Noticeable in the crystalline phase is Whitlockite ( $\text{Ca}_9(\text{MgFe})(\text{PO}_4)_6\text{PO}_3\text{OH}$ ) at 2.33 wt.%, a calcium orthophosphate crystal in which, magnesium is partly substituted for calcium [30]. This is a bio ceramic found in calcified tissue and it is the second most abundant inorganic mineral in living bone [31] and is traceable to the periwinkle shell. Also present is Wollastonite ( $\text{CaSiO}_3$ ) at 6.86 wt.%. The presence of Whitlockite may confer some bioactivity on the glass ceramic. The resurgence of bioactivity in glass ceramics is interesting for biomedical applications because of the prospect of combining the higher bioactivity of glasses over hydroxyapatite [32], with the superior mechanical properties of glass ceramics.

### 3.8 Appearance of glass ceramic bead

The glass ceramic bead is shown in Fig. 17. It has a light yellowish tint, which appears golden under a white spotlight. It is mostly transparent in thin sections; this however decreases in thicker sections. This correlates with the FTIR spectra which showed high transmittance numbers of between 92 and 97%. The relatively high transparency of the glass ceramic is an indication of its significant residual amorphous glassy phase of about 55%. There is always a tradeoff between crystallinity and transparency in glass ceramics; the higher the crystallinity the lower the transparency and vice versa

**Fig. 17** Glass ceramic bead showing a light yellowish tint



[33]. Highly crystalline glass ceramic (above 85%) tend to be significantly opaque. The yellowish appearance could be due to the presence of phosphorus oxides. The EDS data for the glass ceramic indicated the presence of phosphorus (1.6 wt.%). Phosphorus oxide is a colour intensifier in glass and is known to induce a yellowish colour in glass at small concentrations [34].

## 4 Conclusions

The ubiquitous soda-lime glass is commonly made from silicon oxide, calcium oxide and sodium oxide typically sourced from natural reserves. The unbridled consumption of glass making raw materials calls into question their sustainability in the mid to long term. This work demonstrated a high-level utilization of rice husk and periwinkle shells in the production of a glass ceramic. The goal of a “circular economy” can be achieved through the utilization of these environmental wastes, and more value addition infused into the production chain of rice production and periwinkles harvesting. The presence of Whitlockite, a magnesium and phosphorus rich bio ceramic, and wollastonite suggests some bioactive capabilities in the glass ceramic. Furthermore, rice husk can be considered as a viable route for the sourcing of silica for glass making and a range of other industrial applications.

**Acknowledgements** The Authors wish to acknowledge the MSE Alumni laboratories of the Department Materials Science and Engineering, Obafemi Awolowo University for the kind use of their facilities.

**Author contributions** BA carried out all the SEM/EDS analysis and played the lead role in writing the manuscript. Additionally, BA jointly supervised the work with MOA. All the XRD analyses were jointly done by DAI and KMO. Both OEA and OEB collected the rice husk samples and extracted the silica, they also mixed the various other component ingredients and produced the glass ceramic. GFA and SAA collected and processed the periwinkle shells. They also carried out the FTIR and analyzed the FTIR data. BA and MOA reviewed the FTIR data performed editorial checks on the prepared manuscript. All the authors reviewed the manuscript.

**Funding** This research was not supported by any funding entity.

**Data availability** The authors hereby declare that all the data supporting the findings of this study are available within the paper. Should any raw data files be needed in another format, they are available from the corresponding author upon request.

## Declarations

**Competing interests** There are no competing interest in this work.

**Open Access** This article is licensed under a Creative Commons Attribution 4.0 International License, which permits use, sharing, adaptation, distribution and reproduction in any medium or format, as long as you give appropriate credit to the original author(s) and the source,

provide a link to the Creative Commons licence, and indicate if changes were made. The images or other third party material in this article are included in the article's Creative Commons licence, unless indicated otherwise in a credit line to the material. If material is not included in the article's Creative Commons licence and your intended use is not permitted by statutory regulation or exceeds the permitted use, you will need to obtain permission directly from the copyright holder. To view a copy of this licence, visit <http://creativecommons.org/licenses/by/4.0/>.

## References

1. de Lima CJ, Veer F, Çopuroglu O, Nijssse R. Advancements and challenges in glass concepts, manufacturing and applications. In: Paper presented at the 13th International Congress on Advances in Civil Engineering. September 12–14, 2018; Izmir.
2. Jiang ZH, Zhang QY. The formation of glass: a quantitative perspective. *Sci China Mater.* 2015;58:378–425. <https://doi.org/10.1007/s40843-015-0048-z>.
3. Burkowicz A, Galos K, Guzik K. The resource base of silica glass sand versus glass industry development: the case of Poland. *Resources.* 2020;9(0134):1–20. <https://doi.org/10.3390/resources9110134>.
4. Khater GA, Safwat EM, Kang J, Yue Y, Khater AGA. Some types of glass-ceramic materials and their applications. *Int J Res Stud Sci Eng Technol.* 2020;7(3):1–16.
5. Alzahrani AS. A review of glass and crystallizations of glass-ceramics. *Adv Mater Phys Chem.* 2022;12:261–88. <https://doi.org/10.4236/ampc.2022.1211018>.
6. Han L, Song J, Lin C, Liu J, Liu T, Zhang Q, et al. Crystallization, structure and properties of MgO-Al<sub>2</sub>O<sub>3</sub>-SiO<sub>2</sub> highly crystalline transparent glass-ceramics nucleated by multiple nucleating agents. *J Eur Ceram Soc.* 2018;38(13):4533–42. <https://doi.org/10.1016/j.jeurceramsoc.2018.05.025>.
7. Fukagawa NK, Ziska LH. Rice: importance for global nutrition. *J Nutr Sci Vitaminol.* 2019;65:S2–3. <https://doi.org/10.3177/jnsv.65.S2>.
8. Wallach O. This is how much rice is produced around the world - and the countries that grow the most. *Visual Capitalist.* 2022. <https://www.weforum.org/agenda/2022/03/visualizing-the-world-s-biggest-rice-producers/>. Accessed 15 June 2023.
9. Akhter F, Soomro SA, Jamali AR, Chandio ZA, Siddique M, Ahmed M. Rice husk ash as green and sustainable biomass waste for construction and renewable energy applications: a review. *Biomass Conv Bioref.* 2023;13:4639–49. <https://doi.org/10.1007/s13399-021-01527-5>.
10. Madhumita S, Bhattacharyya S, Behera RC. Effect of temperature on morphology and phase transformations of nano-crystalline silica obtained from rice husk. *Phase Transit.* 2009;82(5):377–86. <https://doi.org/10.1080/01411590902978502>.
11. Rozainee M, Ngo SP, Salema AA. Effect of fluidizing velocity on the combustion of rice husk in a bench-scale fluidized bed combustor for the production of amorphous rice husk ash. *Bioresour Technol.* 2008;99:703–13. <https://doi.org/10.1016/j.biortech.2007.01.049>.
12. Pode R. Potential applications of rice husk ash waste from rice husk biomass power plant. *Renew Sustain Energy Rev.* 2016;53:1468–85. <https://doi.org/10.1016/j.rser.2015.09.051>.
13. Musa NA, Akinbode FO. Utilizing rice husk briquettes in firing crucible furnace for low temperature melting metals in Nigeria. *Eng Technol Appl Sci Res.* 2012;2(4):265–8.
14. Jiang S, Xu J, Wang H, Wang X. Study of the effect of pyrite and alkali-modified rice husk substrates on enhancing nitrogen and phosphorus removals in constructed wetlands. *Environ Sci Pollut Res.* 2022;29:54234–49. <https://doi.org/10.1007/s11356-022-19537-9>.
15. Ogungbenle HN, Omowole BM. Chemical, functional and amino acid composition of periwinkle (*Tympanotonus fuscatus* var. *radula*) meat. *Int J Pharm Sci Rev Res.* 2012;13(2):128–32.
16. Dahunsi BIO. Properties of periwinkle-granite concrete. *J Civil Eng.* 2002;8:27–36. <https://doi.org/10.4314/jce.v8i1.18993>.
17. Sadiq A, Abdelmalik AA, Sadiq U, Abdurraheem A, Balogun M. Influence of periwinkle shell microparticle on the mechanical properties of epoxy polymer composite. *Niger Res J Chem Sci.* 2020;8(1):25–6.
18. Aimikhe VJ, Lekia GB. An overview of the applications of periwinkle (*Tympanotonus fuscatus*) shells. *Curr J Appl Sci Technol.* 2021;40(18):31–58. <https://doi.org/10.9734/cjast/2021/v40i1831442>.
19. Nworie CE, Onukwuli DO, Ekebafé LO, Ezeugo JO. Preparation and characterization of periwinkle shell activated carbon. *Niger Res J Chem Sci.* 2020;8(1):244–54.
20. Adzor SA, Nwoke VU, Akaluzia RO. Investigation of the suitability of periwinkle snail shells as carburizing material for the surface hardness improvement of low carbon steel. *Eur J Mater Sci.* 2016;3(2):13–23.
21. Anderson R. Resource depletion: opportunity or looming catastrophe? 2012. <https://www.bbc.com/news/business-16391040>. Accessed on 8 Aug 2023.
22. Hossain SS, Yadav S, Majumdar S, Krishnamurthy S, Pyare R, Roy PK. A comparative study of physico-mechanical, bioactivity and hemolysis properties of pseudo-wollastonite and wollastonite glass-ceramic synthesized from solid wastes. *Ceram Int.* 2020;46(1):833–43.
23. Adam KH, Fua HA. Production of silica from biogenic material. Malaysian Patent MY-136715-A. 2008.
24. Mohamed RM, Mkhaliid IA, Barakat MA. Rice husk ash as a renewable source for the production of zeolite NaY and its characterization. *Arabian J Chem.* 2015;8:48–53. <https://doi.org/10.1016/j.arabjchem.2012.12.013>.
25. Baucio ML. ASM engineered materials reference book. 2nd ed. Abingdon: Taylor and Francis; 1994.
26. Loganathan P, Naidu G, Vigneswaran S. Mining valuable minerals from seawater: a critical review. *Environ Sci Water Res Technol.* 2017;3:37–53. <https://doi.org/10.1039/c6ew00268d>.
27. Torres-Carrasco M, Palomob JG, Puertas F. Sodium silicate solutions from dissolution of glass wastes, statistical analysis. *Mater Constr.* 2014;64(314):1–14. <https://doi.org/10.3989/mc.2014.05213>.
28. Choudhary R, Koppala S, Swamiappan S. Bioactivity studies of calcium magnesium silicate prepared from eggshell waste by sol-gel combustion synthesis. *J Asian Ceram Soc.* 2015;3(2):173–7. <https://doi.org/10.1016/j.jascr.2015.01.002>.
29. Zhang X, Sun Y, Mao Y, Chen K, Cao Z, Qi D. Controllable synthesis of raspberry-like PS-SiO<sub>2</sub> nanocomposite particles via Pickering emulsion polymerization. *RSC Adv.* 2018;8:3910–8.
30. Lagier R, Baud CA. Magnesium whitlockite, a calcium phosphate crystal of special interest in pathology. *Pathol Res Pract.* 2003;199(5):329–35. <https://doi.org/10.1078/0344-0338-00425>.

31. Jang HL, Jin K, Lee J, Kim Y, Nahm SH, Hong KS, et al. Revisiting whitlockite, the second most abundant biomineral in bone: nanocrystal synthesis in physiologically relevant conditions and biocompatibility evaluation. *ACS Nano*. 2014;8(1):634–41. <https://doi.org/10.1021/nn405246h>.
32. Yadav S, Singh P, Pyare R. Synthesis, characterization, mechanical and biological properties of biocomposite based on zirconia containing 1393 bioactive glass with hydroxyapatite. *Ceram Int*. 2020;46(8):10442–51.
33. Patra P, Annapurna K. Transparent tellurite glass-ceramics for photonics applications: a comprehensive review on crystalline phases and crystallization mechanisms. *Prog Mater Sci*. 2022;125: 100890. <https://doi.org/10.1016/j.pmatsci.2021.100890>.
34. Velikanova ÉY, Gorashchenko NG. Effect of phosphorus oxide additives on the color and production conditions of Bi<sub>2</sub>O<sub>3</sub>–SiO<sub>2</sub>–P<sub>2</sub>O<sub>5</sub> glass. *Glass Ceram*. 2011;68:209–10.

**Publisher's Note** Springer Nature remains neutral with regard to jurisdictional claims in published maps and institutional affiliations.